Manuscript prepared for Clim. Past Discuss.
with version 2014/05/30 6.91 Copernicus papers of the LaTeX class copernicus.cls.
Date: 6 February 2015

Comparing past accumulation rate reconstructions in East Antarctic ice cores using ^{10}Be, water isotopes and CMIP5-PMIP3 models

A. Cauquoin[1], A. Landais[1], G. M. Raisbeck[2], J. Jouzel[1], L. Bazin[1], M. Kageyama[1], J.-Y. Peterschmitt[1], M. Werner[3], E. Bard[4], and ASTER Team[4,*]

[1]Laboratoire des Sciences du Climat et de l'Environnement (LSCE/IPSL, CEA-CNRS-UVSQ), CEA Saclay Orme des Merisiers, 91191 Gif-sur-Yvette, France
[2]Centre de Sciences Nucléaires et de Sciences de la Matière (CSNSM), UMR CNRS 8609, Université Paris Sud XI, Bât 108, 91405 Orsay, France
[3]Alfred Wegener Institute for Polar and Marine Research (AWI) Bussestraße 24, 27570 Bremerhaven, Germany
[4]Aix-Marseille Université, CNRS-IRD-Collège de France, UM 34 CEREGE, Technopôle de l'Environnement Arbois-Méditerranée, BP80, 13545 Aix-en-Provence, France
[*]M. Arnold, G. Aumaître, D. L. Bourlès and K. Keddadouche

Correspondence to: A. Cauquoin (Alexandre.Cauquoin@lmd.jussieu.fr)

Abstract

Ice cores are exceptional archives, which allow us to reconstruct a wealth of climatic parameters as well as past atmospheric composition over the last 800 ka in Antarctica. Inferring the variations of past accumulation rate in polar regions is essential both for documenting past climate and for ice core chronology. On the East Antarctic plateau, the accumulation rate is so small that annual layers cannot be identified and accumulation rate is mainly deduced from the water isotopic composition assuming constant temporal relationships between temperature, water isotopic composition and accumulation rate. Such an assumption leads to large uncertainties on the reconstructed past accumulation rate. Here, we use high-resolution beryllium-10 (^{10}Be) as an alternative tool for inferring past accumulation rate for the EPICA Dome C ice core, in East Antarctica. We present a high-resolution ^{10}Be record covering a full climatic cycle over the period 269 to 355 ka from MIS 9 to MIS 10 (Marine Isotope Stages), including a warmer period than preindustrial (MIS 9.3 optimum). After correcting ^{10}Be for the estimated effect of the paleomagnetic field, we deduce that the ^{10}Be reconstruction is in reasonably good agreement with EDC3 values for the full cycle except for the period warmer than present. For the latter, the accumulation is up to 13% larger (4.46 $\mathrm{cm\,ie\,yr^{-1}}$ instead of 3.95). This result is in agreement with the studies suggesting an underestimation of the deuterium-based accumulation for the optimum of the Holocene (Parrenin et al., 2007a). Using the relationship between accumulation rate and surface temperature from the saturation vapour relationship, the ^{10}Be-based accumulation rate reconstruction suggests that the temperature increase between the MIS 9.3 optimum and present-day may be 2.4 K warmer than estimated by the water isotopes reconstruction. We compare these reconstructions to the available model results from CMIP5-PMIP3 for a glacial and an interglacial state, i.e. for the Last Glacial Maximum and pre-industrial climates. While 3 out of 7 models show relatively good agreement with the reconstructions of the accumulation-temperature relationships based on ^{10}Be and water isotopes, the others models either underestimate or overestimate it, resulting in a range of model results much larger than the range of the reconstructions. Indeed, the models can encounter some difficulties to simulate

precipitation changes linked with temperature or water isotope content on the East Antarctic plateau during glacial–interglacial transition and need to be improved in the future.

1 Introduction

Polar ice cores provide reference records for past climatic conditions over the last 130 ka (thousands of years) in Greenland (North Greenland Ice Core Project Members, 2004; NEEM Community Members, 2013) and over the last 800 ka in Antarctica (EPICA Community Members, 2004). That ice as old as 800 ka can be retrieved at a depth of 3200 m is due to the very low accumulation rate encountered at this site of the East Antarctic Plateau (2.73 cm ice equivalent per year today, EPICA Community Members, 2004). Accumulation rate is even smaller during glacial periods as expected from simple thermo-dynamical considerations: cold air holds less moisture than warm air. Still, the quantitative reconstruction of past accumulation rate is not straightforward and large uncertainties ($> 30\,\%$) are often associated with its reconstruction in polar ice cores (Blunier et al., 2007; Guillevic et al., 2013; van Ommen and Morgan, 1997).

Reducing the uncertainties on the reconstruction of past accumulation rate is essential for several reasons. First and most obviously, this will lead to an improved ice core chronology. Second, even if the physical relationship between air moisture content and temperature holds true with time, there is no a priori reason why the link between accumulation rate and temperature should be constant with time in polar regions, at the very end of the water distillation process. Because of the spatial and temporal variations in the origin and trajectories of air masses, some decoupling can be expected between accumulation rate and temperature or water isotopes from which polar temperature is classically retrieved. Finally, the simulation of polar accumulation and of its link with temperature is a weakness for many models so that an evaluation of the modeled relationship between temperature vs. accumulation against accumulation reconstructions is desirable. There is thus a clear need for temperature – and water isotope – independent estimates of past accumulation changes.

An alternate way to reconstruct past accumulation rate is the use of beryllium-10 ($^{10}\mathrm{Be}$), a cosmogenic isotope to obtain an independent estimate of past accumulation. After their pro-

duction in the upper atmosphere (Lal and Peters, 1967), ^{10}Be atoms become fixed to aerosols and fall very quickly (within 1–2 years according to Raisbeck et al., 1981a) on the Antarctic plateau. A simplistic assumption, namely that the ^{10}Be flux is constant through time, has been applied to estimate accumulation changes along the Vostok ice core, first from a limited set of measurements (Yiou et al., 1985) and then from a more detailed, but still low resolution and discontinuous data set covering the last climatic cycle (Jouzel et al., 1989). This assumption was suggested by the anti-correlation observed between ^{10}Be concentrations in ice and accumulation rate derived from oxygen isotopes at the drilling site (Yiou et al., 1985). However, the assumption of a constant ^{10}Be flux is limited by the heliomagnetic and geomagnetic modulations: the higher these fields are, the more primary cosmic ray particles are deflected which leads to a decrease of cosmogenic isotope production. For example, this problem is important for the last glacial period which includes the Laschamp excursion, a dramatic short-lived decrease in the Earth's magnetic field intensity occurring about 41 kyr ago (Singer et al., 2009).

In the present study, we exploit a continuous and very detailed ^{10}Be time series covering a full climatic cycle over a 86 ka-period, from MIS 9 to MIS 10 (Marine Isotope Stages), measured along the Dome C ice core (75°06′ S, 123°21′ E). Two geomagnetic events are mentioned during this time range at 290 ka (so-called "Portuguese Margin" Thouveny et al., 2008) and 320 ka (so-called "Calabrian Ridge 1" Langereis et al., 1997). This 269-355 ka record has been prepared and measured in the framework of the PhD of Cauquoin (2013). It completes a high resolution ^{10}Be record between 170 and 800 ka at EDC that will be published separately (Raisbeck et al., in prep). Two advantages of using the period 269-355 ka for this study are (1) it has the largest glacial-interglacial range of δD and thus estimated temperature and accumulation, (2) it has relatively small geomagnetic variations, as compared for example to last climatic cycle (Blake and Laschamp excursions). Thus the sensitivity of ^{10}Be concentration due to accumulation variations compared to those due to production variations should be particularly favorable.

Our manuscript is organized as follows. After a reminder of the classical estimation of past accumulation rates from water isotopes in ice core and a presentation of the procedure, we examine the multidecadal ^{10}Be record and discuss how this ~ 86 ka long record allows inferences

about the associated glacial–interglacial accumulation rate change. In the following section, we discuss the relationship between temperature/δD and accumulation rate changes on the East Antarctic plateau over deglaciations using constraints both from glaciological data and from 11 modeling outputs inferred from 8 CMIP5-PMIP3 models, plus one simulation (ECHAM5) being equipped with stable water isotope diagnostics for preindustrial (PI) and Last Glacial Maximum (LGM, 21 000 years ago).

2 Methods

2.1 The classical estimation of past accumulation rates from water isotope data on the East Antarctic plateau

The physical link between the moisture content of air mass and its temperature has been systematically used to estimate past accumulation in Antarctica and establish ice core chronologies. This approach linking accumulation rate to temperature has been first proposed by Lorius et al. (1985) and Ritz (1992). Using a simple unidimensional model neglecting the possible changes in circulation intensity over the precipitation area, one infers that the precipitation rate at a time t is given by the equation 1, where A is the accumulation rate, P_{sat} the saturation pressure over ice, and t_0 refers to present-day values:

$$A(t) = A(t_0) \times \frac{[\partial(P_{\text{sat}}/(T+273))/\partial T]_t}{[\partial(P_{\text{sat}}/(T+273))/\partial T]_{t_0}} \quad (1)$$

The temperature considered in Eq. (1) is the temperature at condensation, approximated by the inversion temperature, T_{inv}, itself related to surface temperature T_{s} in Antarctica over a range from -15 to $-55\,^{\circ}\text{C}$ (Jouzel and Merlivat, 1984) by:

$$T_{\text{inv}} = 0.67 \times T_{\text{s}} - 1.2 \quad (2)$$

where T_{s} is the mean near-surface atmospheric temperature either measured at $15\,\text{m}$ deep in the firn or deduced from the average of the measured temperatures at $2\,\text{m}$ height in weather

station. This relation has been confirmed by Connolley (1996) and Ekaykin (2003) for the East Antarctic plateau.

In Antarctica, past temperature changes are classically retrieved from water isotope records in ice cores (δD or δ^{18}O) assuming that the present-day temperature/isotope spatial slope can be taken as a surrogate for the temporal slope at a given site. Using alternative methods to constrain past temperature in polar regions (combination of δ^{18}O and d-excess, Vimeux et al., 2002, use of the isotopic composition of inert gases combined with firnification models, Caillon et al., 2001, borehole temperature inversion, Salamatin et al., 1998), it has been shown that errors associated with this conventional approach are estimated to be of -10 to $+30$ % over glacial–interglacial transitions (Jouzel et al., 2003). However, a recent modelling experiment has suggested that error on the temperature reconstruction can reach up to 100 % for warmer interglacial periods (Sime et al., 2009).

The classical method for temperature reconstruction applied to sites in East Antarctica like Vostok, (Jouzel et al., 1987; Petit et al., 1999), Dome F (Watanabe et al., 2003) and EPICA Dome C (Jouzel et al., 2007), assumes that the temporal variations of δD, $\Delta\delta D$, are proportional to the temporal variations of surface temperature, ΔT_{surf}:

$$\Delta\delta D = 6.04 \times \Delta T_{\text{surf}} \tag{3}$$

Here the temperatures are expressed in °C.

The saturation vapour pressure over ice is linked with temperature and can be approximated in the range -70 °C to 0 °C by the following equation (Wagner and Pruß, 2002):

$$P_{\text{sat}}(T) = A \times 10^{\frac{mT}{T+T_n}} \tag{4}$$

with $A = 6.114742$, $m = 9.778707$ and $T_n = 273.1466$.

From the numerical solution of Eqs. (1) to (4) over the range of temperature variations observed in East Antarctica ice cores, it appears that the accumulation rate is almost exponentially linked to temperature. Indeed, the Clausius-Clapeyron relation determines that the water-holding capacity of the atmosphere increases by about 7% for every 1 degree rise in temperature.

Keeping this idea of an exponential link, Parrenin et al. (2007a) and Bazin et al. (2013) have formulated the accumulation/isotope relation as:

$$A = A_0 \exp(\beta \Delta \delta D) \quad (5)$$

where A_0 is an estimate of the present-day accumulation rate and β an adjustable parameter which is optimized during the chronology construction through chronological control points and an ice flow model (Parrenin et al., 2007b). While the accumulation rate reconstruction should be rather accurate for the upper part of the ice core, the uncertainties increase with depth because less chronological constraints are available and ice thinning becomes less predictable.

For the estimate of accumulation rate at Dome C with the EDC3 timescale, Parrenin et al. (2007a, b) have used an inverse method in order to get the best fit with a series of age markers (listed in Table 3 of Parrenin et al., 2007a). They have inferred the value of β in Eq. (5) as being equal to 0.0157, a value about 50 % higher than the one (0.0102) corresponding to the saturation vapour assumption (e.g. as derived from Eq. (1) and compared to the EDC3 accumulation rate on Fig. 2a).

More recently, during the construction of the AICC2012 chronology, the imposed relationship between δD and accumulation rate has been relaxed. The AICC2012 timescale (Bazin et al., 2013; Veres et al., 2013) has been developed for obtaining a coherent chronology between one Greenland ice core (NorthGRIP) and four Antarctic ice cores (EDC, EDML, TALDICE, Vostok) through the intensive use of relative tie points in the ice and gas phases of the different ice cores. In the chronological optimization process of AICC2012 performed by the DATICE Bayesian dating tool (Lemieux-Dudon et al., 2010), the scenario for both accumulation rate and thinning function for the different ice cores are allowed to vary freely, i.e. without an imposed relationship between accumulation rate and water isotopes as for the EDC3 chronology. Although the background scenario for EDC accumulation rate is the one given by Eq. (1), it is associated with a relatively large variance so that it is easily modified during the chronology optimization process. At the end, the amplitude of glacial–interglacial variations of accumulation rate over Termination 4 at Dome C is 5 % smaller in AICC2012 than in EDC3 (Fig. 2b).

2.2 ^{10}Be measurements

The first procedure for measuring $^{10}\mathrm{Be}$ in ice cores was described by Raisbeck et al. (1981b). Since then, efficiency has been greatly improved, both due to improvement of chemical procedures of the samples and AMS (Accelerator Mass Spectrometry) techniques (Raisbeck et al., 1987, 2007; Yiou et al., 1997). The ice from the Dome C ice core available for this study is a continuous series of "bag samples" (each measuring 55 cm) between 2384 and 2627 m deep. Each bag sample was cut into five pieces of 11 cm (weighting $\sim 50\,\mathrm{g}$) in order to obtain a high resolution $^{10}\mathrm{Be}$ profile. This corresponds to around 2200 samples. The preparation of the samples was made at the Centre de Sciences Nucléaires et de Sciences de la Matière (CSNSM) in Orsay.

The current chemical procedure is described by Raisbeck et al. (2007). The samples were melted in a centrifuge cone, in the presence of 0.25 mg of $^{9}\mathrm{Be}$ carrier. The $\mathrm{Be(OH)_2}$ was then directly precipitated with ammonia ($\mathrm{NH_4OH}$). The precipitate was extracted by centrifugation, then dissolved with 250 µL of nitric acid and 500 µL of highly pure water. The solution was transferred to a ceramic crucible to be dried on a hotplate and then heated to 900 °C during 45 min over an electric furnace in order to transform the precipitate to BeO. The beryllium oxyde was mixed with Niobium (Nb) powder and pressed into a copper cathode. The $^{10}\mathrm{Be}/^{9}\mathrm{Be}$ measurements were carried out at the ASTER (Accélérateur pour les Sciences de la Terre, Environnement, Risques) AMS facility at the Centre Européen de Recherche et d'Enseignement des Géosciences de l'Environnement (CEREGE) in Aix-en-Provence (Arnold et al., 2010), relative to the NIST (National Institute of Standards and Technology) Standard Reference Material (SRM) 4325, using the certified ratio of 2.68×10^{-11} $^{10}\mathrm{Be}/^{9}\mathrm{Be}$. We are aware that many people now use the value of 2.79×10^{-11} given by Nishiizumi et al. (2007) for this standard. We have continued to use the value of 2.68 because it was in excellent agreement with the original home-made standard of the Orsay group (Raisbeck et al., 1978), and has been used for all our previous measurements. If desired, a conversion can be easily made, and will have no effect on relative values. The isobar $^{10}\mathrm{B}$ is suppressed by use of an absorber foil in the rare isotope path (Klein et al., 2008). The counting statistics lead to an uncertainty of typically 4 % for 1σ

standard deviation. The chemical blanks produced with our ^{9}Be carrier used for the ice samples yielded an average process background $^{10}\mathrm{Be}/^{9}\mathrm{Be}$ of $(3.95 \pm 2.35) \times 10^{-15}$. In comparison, the $^{10}\mathrm{Be}/^{9}\mathrm{Be}$ ratios measured for EDC samples were on the order of 3.2×10^{-13}.

2.3 Models

In this study, we also want to test our experimental results by comparing them with the latest climate simulations of the LGM and PI climates, obtained in the framework of the PMIP3 and CMIP5 projects (Braconnot et al., 2012). Both the PI and LGM climate simulations are equilibrium simulations, i.e. obtained by imposing non-evolving boundary conditions and forcings. Compared to the pre-industrial control simulations, LGM climate simulations are obtained by imposing the LGM ice sheet reconstructions (topography, albedo and land–sea mask differences due to sea-level lowering), the LGM atmospheric concentration of the main greenhouse gases as recorded by ice-cores and orbital forcing parameters for 21 000 years before present (following Berger, 1978). The experimental set-up is described in detail in the PMIP3 web site: http://pmip3.lsce.ipsl.fr/. The simulations used in this study are those which were available on the CMIP5 database as of October 2012.

In addition to the CMIP5-PMIP3 atmosphere-ocean coupled simulations we are using preindustrial and LGM simulation results obtained from the AGCM (Atmospheric General Circulation Model) ECHAM5 (Roeckner et al., 2006) enhanced with stable water isotope diagnostics (Werner et al., 2011). For the LGM climate simulation, PMIP3-conform boundary conditions have been applied. Glacial sea surface temperatures and sea ice coverage has been derived from the GLAMAP Atlantic reconstruction data set (Schäfer-Neth and Paul, 2003). Both PI and LGM simulation have been performed with a fine T106L31 spectral model resolution (horizontal grid box size of approx. $1.1^\circ \times 1.1^\circ$, 31 vertical levels).

All CMIP5-PMIP3 simulations are summarized in Table 1. From the different simulations we have used the following variables: tas (near surface air temperature) and pr (precipitation rate). As the sublimation rate was only available for 3 models out of 11 and as its values over the sites of interest were negligible compared to the precipitation rate in these models, we have not included the sublimation rate in the calculation of the accumulation rate changes from

LGM to PI. We observe that tas is systematically higher than the measured mean atmospheric temperature, which is a typical bias of CMIP5-PMIP3 simulations in polar regions (see Risi et al., 2010). To evaluate the consequences of this bias, we have extracted the modeled inversion temperatures available in the IPSL-CM5A-LR model. These data show that in the models, the slope of the relationship between tas and the modeled inversion temperature is 15 % higher than the one given by Jouzel and Merlivat (1984) (cf. Eq. 2). However, when we use the modeled surface temperature T_{sm} (which is on average 4 °C lower than the simulated tas values), we obtain a slope between T_{inv} and T_{sm} very close to the observed value of 0.67 (see Eq. 2). As a consequence and to artificially compensate for the cold bias of the CMIP5-PMIP3 simulations, we have extracted both tas and T_{sm} for the following calculations.

For all the models, the values of the LGM–PI change in near-surface air temperature and precipitation rate are obtained by averaging the values of temperature and precipitation on a box of latitudes 77.6 to 72.6 °S and longitudes 120.85 to 125.85 °E.

3 From ^{10}Be concentrations to accumulation rate reconstruction

Figure 1a shows the high-resolution profile of $^{10}\mathrm{Be}$ concentrations (available as supplementary material at doi:10.5194/cpd-0-1-2015-supplement). The time resolution for the shown period varies between 20 years for MIS 9.3 and 70 years for MIS 10, the glacial period older than 340 ka (Fig. 1f). In this study, we will mainly focus on the transition between the coldest part of the MIS 10 reached just before Termination IV and MIS 9.3. The MIS 10 glacial maximum between 341.77 and 348.41 ka (light blue area on Fig. 1b) is at the same water isotopic level as the LGM (Jouzel et al., 2007). Then, MIS 9.3 can be decomposed in two phases: (1) a period with a higher isotopic level than PI with an optimum between 332.55 and 334.53 ka (light red area on Fig. 1b) and (2) a plateau between 325.92 and 330.92 ka at the same isotopic level than PI (light yellow area on Fig. 1b).

We observe a strong anti-correlation between $^{10}\mathrm{Be}$ concentration (Fig. 1a) and δD or δD-derived accumulation rate (Fig. 1b). This is not unexpected since $^{10}\mathrm{Be}$ reaches the Antarctic plateau primarily by dry deposition so concentration of $^{10}\mathrm{Be}$ in the ice is reduced for high accu-

mulation periods. It has thus been proposed that ^{10}Be flux is a more appropriate parameter than concentration for estimating variations in ^{10}Be production (Yiou et al., 1985). This is illustrated in Fig. 1c showing the ^{10}Be flux $F[^{10}\mathrm{Be}]$ as obtained by multiplying the ^{10}Be concentration $C[^{10}\mathrm{Be}]$ times the accumulation rate A from the EDC3 timescale (Parrenin et al., 2007a, b) and the density of ice ρ as:

$$F[^{10}\mathrm{Be}] = C[^{10}\mathrm{Be}] \times A \times \rho \tag{6}$$

Other potential contributions to ^{10}Be concentration variations are linked to (1) variations in the geomagnetic field intensity over centennial to millennial scales or (2) variations in the solar activity on decadal to centennial timescales. For the influence of the relative changes of geomagnetic field, we can make corrections by using independent estimates of the field intensity obtained by a stacked record of marine sediments (Channell et al., 2009). We assume that our ^{10}Be flux record reflects the globally averaged ^{10}Be production. We have also carried out the calculations using the "polar bias" assumption (polar ^{10}Be flux 20% less sensitive to geomagnetic field intensity changes (Field et al., 2006), i.e. we multiply the relative variations of the ^{10}Be flux by 0.8), with a negligible difference in the resulting accumulation reconstructions. After synchronizing the time scale of the marine record with that of EDC (Cauquoin, 2013), we apply the theoretical estimate of Masarik and Beer (2009) on the relationship between ^{10}Be production and geomagnetic intensity, as shown in Fig. 1d. Then, we divide the ^{10}Be flux at EDC by the relative changes of global ^{10}Be production according to PISO-1500. The main effect of this correction is to remove the long term decrease in the uncorrected ^{10}Be flux from 270 to 350 ka (Fig. 1e). We have also looked at the theoretical estimate of Kovaltsov and Usoskin (2010) on the relationship between ^{10}Be production and geomagnetic field intensity, with very similar results.

Since we have no independent estimate of the solar variability during the time period being studied, we must assume that the average value of solar activity has been constant during this time. In reality, some of the remaining centennial structure in the ^{10}Be flux of Fig. 1e may be due to variations of solar activity, or to centennial geomagnetic variations not recorded by the marine cores. We now use the geomagnetically corrected ^{10}Be flux curve of Fig. 1e to estimate the

ice accumulation rate of EDC during our time period using equation 6. This procedure assumes that the spatial distribution of geomagnetically corrected ^{10}Be deposition remains constant with time independent of climate and type of deposition. While it is difficult to give a quantitative uncertainty of our constant flux assumption, we can note that the 1σ standard deviation of the smooth corrected flux in Fig. 1e is 8.8%. Since this is significantly larger than the analytical uncertainty, it must represent essentially the sum of inadequately corrected production variations plus variability in the ^{10}Be deposition. It thus does not seem unreasonable to conclude that this represents an upper limit to the deposition variability.

In a first attempt to use ^{10}Be for such a reconstruction, we have chosen to keep the exponential link between accumulation and δD. Starting from the formulation proposed by Parrenin et al. (2007a), we have tried to adjust β in order to minimize the variance of the ^{10}Be flux signal while keeping consistency with the time scale of EDC3 (Fig. 2c). For this minimization, we have applied first a 100 year resampling to the ^{10}Be record. Using equations 5 and 6 with A the EDC3 accumulation rate from Parrenin et al. (2007a, b) and A_0 = 2.841 $\mathrm{cm\,ie\,yr^{-1}}$, we have calculated the variance of the ^{10}Be flux (previously corrected for geomagnetic field intensity changes) using different values of β. The variance of the ^{10}Be flux is minimized for a β of 0.0165 (the variance varies less than 1% for values of β between 0.0160–0.0171). This value is 5 % larger than used by Parrenin et al. (2007a), and corresponds to a larger glacial–interglacial amplitude by the same amount. We also notice a general decrease of the variance by a factor 0.99 which supports this revision of accumulation rate estimate from δD over this glacial–interglacial cycle.

In a second attempt, we have performed a test with the assumption of a strictly constant ^{10}Be flux, after a geomagnetic field intensity correction on the ^{10}Be concentration in the ice. We have deduced the resulting accumulation by dividing the ^{10}Be flux $F[^{10}\mathrm{Be}]$ (= 53.44 at.m^{-2}.s^{-1} here) by the ^{10}Be concentration (corrected for radioactive decay and geomagnetic modulation) $C[^{10}\mathrm{Be}]$ times the ice density ρ according to equation 6. The inferred accumulation is reported in Fig. 2d. The general shape of the accumulation rate reconstruction follows the evolution of the EDC3 accumulation rate. However, while there is no significant difference in the accumulation reconstruction between the MIS 10 glacial maximum and the plateau of the MIS 9.3

(increase of 1.548 for the ^{10}Be-based accumulation rate reconstruction and of 1.624 $\mathrm{cm\,ie\,yr^{-1}}$ for EDC3), there is a clear difference for accumulation rate increase between the plateau and the MIS 9.3 optimum (1.364 $\mathrm{cm\,ie\,yr^{-1}}$ for the ^{10}Be-based reconstruction against 0.920 $\mathrm{cm\,ie\,yr^{-1}}$ for EDC3). The ^{10}Be-based accumulation rate for the latter is up to 13% larger than the EDC3 reconstruction (4.46 $\mathrm{cm\,ie\,yr^{-1}}$ instead of 3.95).

Even if the assumption of a strictly constant ^{10}Be flux is not realistic, we have tested if the inferred accumulation rate is consistent with chronological constraints (Table 2). For this aim, we have imposed this accumulation rate as a background accumulation rate scenario for EDC in the DATICE tool for chronology optimization with a very small associated variance. The other background scenarios for the 4 other ice cores (NorthGRIP, EDML, Taldice, Vostok) are kept identical as those of AICC2012 (Bazin et al., 2013; Veres et al., 2013). In this DATICE experiment, we still use the same 5 ice cores as in AICC2012 for facilitating the comparison with previous chronological studies but for our period of interest, only Vostok goes back until MIS 9/10 and can influence the chronology of EDC. With such background accumulation rate for EDC, the minimization of DATICE is easily reached with very small modifications of the thinning function, well within the imposed variance, compared to the AICC2012 chronology. We find the same trends on the resulting accumulation rate as for the ^{10}Be-based one.

We conclude that both methods show an underestimation of accumulation deduced from water isotopes for the optimum of MIS 9.3. This is in agreement with the study of Parrenin et al. (2007a), which suggested that the deuterium-based reconstruction underestimates accumulation for the optimum of the Holocene. However the existence of a strong link between past changes in accumulation and temperature is confirmed to first order by our ^{10}Be approach and we next examine how paleoclimate simulations performed with different GCMs might reveal further insight on this link between accumulation and temperature.

4 Accumulation vs. temperature/δD relationship in East Antarctica

We compare the outputs from the models described in Sect. 2.3, with the accumulation rate reconstruction presented in the previous section.

Figure 3a shows a compilation of accumulation rate and temperature change for the 11 different simulations included in the CMIP5-PMIP3 coupled models plus ECHAM5, between the LGM and the PI. We have chosen to focus only on the relationship between the change in accumulation rate and the change in temperature between the LGM and PI. Indeed, we can hardly discuss absolute levels of temperature and accumulation rate for two reasons. First, the CMIP5-PMIP3 models are known to overestimate temperature on the East Antarctic plateau. Second, our $^{10}\mathrm{Be}$ data are not covering the last deglaciation as the model simulations but the transition occurring between MIS 10 and the optimum of MIS 9.3 which has larger associated temperature and accumulation rate increases than the last deglaciation (Fig. 3a). Still the accumulation rate vs. temperature slope reconstructed from water isotopes in the ice core (equations 5 and 3 respectively) is almost the same for the transition between MIS 10 and MIS 9 and the last deglaciation as shown in Fig. 3a. We have also checked that the model results shown on Fig. 3a do not change if we replace the ΔT_s calculation based on the near-surface air temperature (tas) by one based on surface temperature (T_sm). Finally, we have tested with the IPSL-CM5A-LR model the influence of the topography changes on the temperature vs. accumulation rate slope by keeping an identical Antarctic ice cap for the LGM and PI conditions and verifying that the relationship remains the same.

We observe a relatively good agreement between the slope of accumulation vs. temperature over a glacial–interglacial transition of several models (MPI-ESM-P, CCSM4, FGOALS-g2), with an average slope of $0.23\,\mathrm{cm\,ie\,yr^{-1}\,{}^{\circ}C^{-1}}$ (bold black line in Fig. 3a). Other models are clearly outside the range of reconstructed accumulation-temperature relationship, either because they overestimate it (MRI-GCM3, GISS-E2-R), underestimate it (IPSL-CM5-LR) or because they simulate very weak changes (CNRM-CM5). Indeed, one can notice a large spread between the different model outputs. The difference in the accumulation rate vs. temperature relationship between different GCM simulations is much larger (100 %) than for the different reconstructions based on $^{10}\mathrm{Be}$ flux and/or chronological constraints. The slope based on the relationship between accumulation rate and saturation pressure over ice is 28 % lower (brown line on Fig. 3a). We conclude that generally the CMIP5-PMIP3 models have more or less difficul-

ties to accurately simulate the temperature-accumulation relationship on the Antarctic plateau between glacial and interglacial conditions and need to be improved in the future.

To avoid any assumption on the relationship between water isotopes and temperature, we have directly compared the accumulation rate with water isotope variations for both ice core data and model outputs (Fig. 3b). In our study, only one model (ECHAM5) is equipped with water isotopes diagnostics. As it was also observed for the temperature change, the δD increase during the deglaciation is smaller in the ECHAM5 simulations than in ice core records. However the slope of accumulation rate vs. δD given by ECHAM5 compares very well with our different accumulation rate vs. δD slope inferred from both water isotopes and $^{10}\mathrm{Be}$. Only the slope deduced from the saturation vapour pressure formulation is lower by $\sim 30\,\%$ compared to EDC3. We observe however that the accumulation rate vs. temperature changes slope of ECHAM5 is smaller than the one reconstructed from water isotopes or $^{10}\mathrm{Be}$ in ice core, and so that the modelled Antarctic δD – temperature gradient in ECHAM5 for LGM – PI climate changes at EDC is much lower than the local geographical gradient as already shown in previous studies (Schmidt et al., 2007; Lee et al., 2008; Sime et al., 2008, 2009). This could imply a problem in the estimation of the surface temperature with measured δD, or also indicate that the δD–temperature slope is under-evaluated in the model compared to the hypothesis of the spatial relationship between precipitation isotopic composition and local temperature (Lorius et al., 1969). But given the uncertainties and the lack of models equipped with water isotope diagnostics, it is difficult to conclude on this point. Finally, this implies that the models matching the accumulation vs. temperature relationship of EDC3 for the last glacial–interglacial change would not necessarily reproduce accurately the associated accumulation rate vs. δD slope.

Finally, an important result highlighted in our study is a possible underestimation of accumulation rate during periods warmer than today as already suggested by Parrenin et al. (2007a) for the optimum of the Holocene. This cannot be tested with the compilation of model outputs displayed here that were only run on colder conditions than preindustrial. Using the relationship between accumulation rate and surface temperature from the saturation vapour formulation, the $^{10}\mathrm{Be}$-based accumulation rate reconstruction suggests that the temperature increase between the plateau and the MIS 9.3 optimum is underestimated by 2.4 K with respect to water isotopes

reconstruction (5.7 vs. 3.2 K). This is in line with the 3 K underestimation for the peak of the last Antarctic interglacial temperature from the relationship between temperature and surface snow isotopic composition as shown in Sime et al. (2009) suggesting an underestimation of about a factor of 2 for warm interglacials compared to a level similar to present day. Instead, the temporal slope is less affected e.g. by about 30% when comparing the plateau (similar to present-day) to MIS 10 glacial maximum (similar to the LGM). Indeed, using the ^{10}Be-based accumulation rate reconstruction and the saturation vapour relationship between accumulation rate and surface temperature leads to an underestimation of the temperature difference between the MIS 10 glacial maximum and the plateau by the water isotopes reconstruction by 25% only (10.2 K vs. 8.2 K). This value is however in the upper range of the interval -10 to + 30% estimated from different approaches by Jouzel et al. (2003). We should keep in mind that these estimates rely on a close relationship between the derivative of the saturation vapour pressure and accumulation change, which is subject to large uncertainties.

5 Conclusions

We have produced the first record of ^{10}Be concentration at high resolution in an ice core over a whole climatic cycle (355 to 269 ka), including a warmer period than preindustrial. After correction for geomagnetic intensity changes, it is generally assumed that the variations in ^{10}Be concentration are mainly linked to variations in the accumulation rate of snow. We have used this property to reconstruct the past accumulation rate at EDC and to compare it with the deuterium-based accumulation rate reconstruction. We have deduced that the ^{10}Be reconstruction is in reasonably good agreement with EDC3 values for the full cycle except the period warmer than present. For the latter, the accumulation is up to 13% larger (4.46 $\mathrm{cm\,ie\,yr^{-1}}$ instead of 3.95). This is in agreement with the study of Parrenin et al. (2007a) who suggested that accumulation rate reconstruction from water isotopes underestimates accumulation for the optimum of the Holocene. Using the relationship between accumulation rate and surface temperature from the saturation vapour formulation, the ^{10}Be-based accumulation rate reconstruction suggests that the temperature increase between the MIS 9.3 optimum and present-day may be under-

estimated by 2.4 K with respect to the water isotopes reconstruction. Finally, the relationship between temperature and accumulation rate is comparable when using the different reconstructions and 4 out of 12 (3 out of 7 models) CMIP5-PMIP3 simulations for LGM–PI climate changes. However, we have noticed a large spread in the model outputs. We conclude that the CMIP5-PMIP3 models can encounter some difficulties to simulate precipitation changes linked with temperature or water isotope content on the Antarctic plateau during large climatic shifts and need to be improved in the future.

Acknowledgements. We acknowledge F. Parrenin, L. Sime and one anonymous referee for their useful comments that helped to improve this manuscript. This work is a contribution to the European Project for Ice Coring in Antarctica (EPICA), a joint European Science Foundation/European Commission (EC) scientific programme, funded by the EC and by national contributions from Belgium, Denmark, France, Germany, Italy, the Netherlands, Norway, Sweden, Switzerland and the UK. The main logistic support was provided by IPEV and PNRA. We acknowledge the World Climate Research Programme's Working Group on Coupled Modelling, which is responsible for CMIP and the Paleoclimate Modelling Intercomparison Project (PMIP). We thank the climate modeling groups (listed in Table 1 of this paper) for producing and making available their model output. For CMIP the US Department of Energy's Program for Climate Model Diagnosis and Intercomparison provides coordinating support and led development of software infrastructure in partnership with the Global Organization for Earth System Science Portals. This work was funded by the French ANR project Dome A and the ERC Grant COMBINISO project no. 306045. The ASTER AMS national facility (CEREGE, Aix en Provence) is supported by the INSU/CNRS, the ANR through the "Projets thématiques d'excellence" program for the "Equipements d'Excellence" ASTER-CEREGE action, IRD, and CEA.

References

Arnold, M., Merchel, S., Bourlès, D. L., Braucher, R., Benedetti, L., Finkel, R. C., Aumaître, G., Gottdang, A., and Klein, M.: The French accelerator mass spectrometry facility ASTER: improved performance and developments, Nucl. Instrum. Meth. B, 268, 1954–1959, doi:10.1016/j.nimb.2010.02.107, 2010.

Bazin, L., Landais, A., Lemieux-Dudon, B., Toyé Mahamadou Kele, H., Veres, D., Parrenin, F., Martinerie, P., Ritz, C., Capron, E., Lipenkov, V., Loutre, M.-F., Raynaud, D., Vinther, B., Svensson, A.,

Rasmussen, S. O., Severi, M., Blunier, T., Leuenberger, M., Fischer, H., Masson-Delmotte, V., Chappellaz, J., and Wolff, E.: An optimized multi-proxy, multi-site Antarctic ice and gas orbital chronology (AICC2012): 120–800 ka, Clim. Past, 9, 1715–1731, doi:10.5194/cp-9-1715-2013, 2013.

Berger, A. L.: Long-term variations of daily insolation and quaternary climatic changes, J. Atmos. Sci., 35, 2362–2367, doi:10.1175/1520-0469(1978)035<2362:LTVODI>2.0.CO;2, 1978.

Blunier, T., Spahni, R., Barnola, J.-M., Chappellaz, J., Loulergue, L., and Schwander, J.: Synchronization of ice core records via atmospheric gases, Clim. Past, 3, 325–330, doi:10.5194/cp-3-325-2007, 2007.

Braconnot, P., Harrison, S. P., Kageyama, M., Bartlein, P. J., Masson-Delmotte, V., Abe-Ouchi, A., Otto-Bliesner, B., and Zhao, Y.: Evaluation of climate models using palaeoclimatic data, Nature Climate Change, 2, 417–424, doi:10.1038/nclimate1456, 2012.

Caillon, N., Severinghaus, J. P., Barnola, J.-M., Chappellaz, J., Jouzel, J., and Parrenin, F.: Estimation of temperature change and of gas age-ice age difference, 108 kyr B. P., at Vostok, Antarctica, J. Geophys. Res., 106, 31893, doi:10.1029/2001JD900145, 2001.

Cauquoin, A.: Flux de ^{10}Be en Antarctique durant les 800 000 dernières années et interprétation, Ph.D. thesis, Université Paris-Sud 11, 2013.

Channell, J. E. T., Xuan, C., and Hodell, D. A.: Stacking paleointensity and oxygen isotope data for the last 1.5 Myr (PISO-1500), Earth Planet. Sc. Lett., 283, 14–23, doi:10.1016/j.epsl.2009.03.012, 2009.

Connolley, W. M.: The Antarctic temperature inversion, Int. J. Climatol., 16, 1333–1342, doi:10.1002/(SICI)1097-0088(199612)16:12<1333::AID-JOC96>3.3.CO;2-Y, 1996.

Ekaykin, A.: Meteorological regime of central Antarctica and its role in the formation of isotope composition of snow thickness, Ph.D. thesis, Université Joseph Fourier – Grenoble I, 2003.

EPICA Community Members: Eight glacial cycles from an Antarctic ice core, Nature, 429, 623–628, doi:10.1038/nature02599, 2004.

Field, C. V., Schmidt, G. A., Koch, D., and Salyk, C.: Modeling production and climate-related impacts on ^{10}Be concentration in ice cores, J. Geophys. Res., 111, D15107, doi:10.1029/2005JD006410, 2006.

Guillevic, M., Bazin, L., Landais, A., Kindler, P., Orsi, A., Masson-Delmotte, V., Blunier, T., Buchardt, S. L., Capron, E., Leuenberger, M., Martinerie, P., Prié, F., and Vinther, B. M.: Spatial gradients of temperature, accumulation and δ^{18}O-ice in Greenland over a series of Dansgaard–Oeschger events, Clim. Past, 9, 1029–1051, doi:10.5194/cp-9-1029-2013, 2013.

Jouzel, J. and Merlivat, L.: Deuterium and oxygen 18 in precipitation: modeling of the isotopic effects during snow formation, J. Geophys. Res., 89, 11749, doi:10.1029/JD089iD07p11749, 1984.

Jouzel, J., Genthon, C., Lorius, C., Petit, J. R., and Barkov, N. I.: Vostok ice core – a continuous isotope temperature record over the last climatic cycle (160,000 years), Nature, 329, 403–408, doi:10.1038/329403a0, 1987.

Jouzel, J., Raisbeck, G., Benoist, J. P., Yiou, F., Lorius, C., Raynaud, D., Petit, J. R., Barkov, N. I., Korotkevitch, Y. S., and Kotlyakov, V. M.: A comparison of deep Antarctic ice cores and their implications for climate between 65,000 and 15,000 years ago, Quaternary Res., 31, 135–150, doi:10.1016/0033-5894(89)90003-3, 1989.

Jouzel, J., Vimeux, F., Caillon, N., Delaygue, G., Hoffmann, G., Masson-Delmotte, V., and Parrenin, F.: Magnitude of isotope/temperature scaling for interpretation of central Antarctic ice cores, J. Geophys. Res., 108, 4361, doi:10.1029/2002JD002677, 2003.

Jouzel, J., Masson-Delmotte, V., Cattani, O., Dreyfus, G., Falourd, S., Hoffmann, G., Minster, B., Nouet, J., Barnola, J.-M., Blunier, T., Chappellaz, J., Fischer, H., Gallet, J. C., Johnsen, S., Leuenberger, M., Loulergue, L., Luethi, D., Oerter, H., Parrenin, F., Raisbeck, G., Raynaud, D., Schilt, A., Schwander, J., Delmo, E., Souchez, R., Spahni, R., Stauffer, B., Steffensen, J. P., Stenni, B., Stocker, T. F., Tison, J. L., Werner, M., and Wolff, E.: Orbital and millennial Antarctic climate variability over the past 800,000 years, Science, 317, 793–796, doi:10.1126/science.1141038, 2007.

Klein, M. G., Gottdang, A., Mous, D. J. W., Bourlès, D. L., Arnold, M., Hamelin, B., Aumaitre, G., Braucher, R., Merchel, S., and Chauvet, F.: Performance of the HVE 5 MV AMS system at CEREGE using an absorber foil for isobar suppression, Nucl. Instrum. Meth. B, 266, 1828–1832, doi:10.1016/j.nimb.2007.11.077, 2008.

Kovaltsov, G. A. and Usoskin, I. G.: A new 3D numerical model of cosmogenic nuclide ^{10}Be production in the atmosphere, Earth Planet. Sc. Lett., 291, 182–188, doi:10.1016/j.epsl.2010.01.011, 2010.

Lal, D. and Peters, B.: Cosmic ray produced radioactivity on the Earth, in: Kosmische Strahlung II/Cosmic Rays II, edited by: Sittle, K., vol. 46/2 of Handbuch der Physik, Springer-Verlag, Berlin, doi:10.1007/978-3-642-46079-1_7, 551–612, 1967.

Langereis, C. G., Dekkers, M. J., Lange, G. J., Paterne, M., and Santvoort, P. J. M.: Magnetostratigraphy and astronomical calibration of the last 1.1 Myr from an eastern Mediterranean piston core and dating of short events in the Brunhes, Geophys. J. Int., 129, 75–94, doi:10.1111/j.1365-246X.1997.tb00938.x, 1997.

Lee, J.-E.., Fung, I., DePaolo, D. J., and Otto-Bliesner, B.: Water isotopes during the Last Glacial Maximum: New general circulation model calculations, J. Geophys. Res., 113, D19109, doi:10.1029/2008JD009859, 2008.

Lemieux-Dudon, B., Blayo, E., Petit, J.-R., Waelbroeck, C., Svensson, A., Ritz, C., Barnola, J.-M., Narcisi, B. M., and Parrenin, F.: Consistent dating for Antarctic and Greenland ice cores, Quaternary Sci. Rev., 29, 8–20, doi:10.1016/j.quascirev.2009.11.010, 2010.

Lipenkov, V. Y., Raynaud, D., Loutre, M. F., and Duval, P.: On the potential of coupling air content and O_2/N_2 from trapped air for establishing an ice core chronology tuned on local insolation, Quaternary Sci. Rev., 30, 3280–3289, doi:10.1016/j.quascirev.2011.07.013, 2011.

Lorius, C., Merlivat, L., and Hagemann, R.: Variation in the mean deuterium content of precipitations in Antarctica, J. Geophys. Res., 74, 7027–7031, doi:10.1029/JC074i028p07027, 1969.

Lorius, C., Ritz, C., Jouzel, J., Merlivat, L., and Barkov, N. I.: A 150,000-year climatic record from Antarctic ice, Nature, 316, 591–596, doi:10.1038/316591a0, 1985.

Masarik, J. and Beer, J.: An updated simulation of particle fluxes and cosmogenic nuclide production in the Earth's atmosphere, J. Geophys. Res., 114, D11103, doi:10.1029/2008JD010557, 2009.

NEEM Community Members: Eemian interglacial reconstructed from a Greenland folded ice core, Nature, 493, 489–494, doi:10.1038/nature11789, 2013.

Nishiizumi, K., Imamura, M., Caffee, M. W., Southon, J. R., Finkel, R. C., and McAninch, J.: Absolute calibration of ^{10}Be AMS standards, Nucl. Instrum. Meth. B, 258, 403–413, doi:10.1016/j.nimb.2007.01.297, 2007.

North Greenland Ice Core Project Members: High-resolution record of Northern Hemisphere climate extending into the last interglacial period, Nature, 431, 147–151, doi:10.1038/nature02805, 2004.

Parrenin, F., Dreyfus, G., Durand, G., Fujita, S., Gagliardini, O., Gillet, F., Jouzel, J., Kawamura, K., Lhomme, N., Masson-Delmotte, V., Ritz, C., Schwander, J., Shoji, H., Uemura, R., Watanabe, O., and Yoshida, N.: 1-D-ice flow modelling at EPICA Dome C and Dome Fuji, East Antarctica, Clim. Past, 3, 243–259, doi:10.5194/cp-3-243-2007, 2007a.

Parrenin, F., Barnola, J.-M., Beer, J., Blunier, T., Castellano, E., Chappellaz, J., Dreyfus, G., Fischer, H., Fujita, S., Jouzel, J., Kawamura, K., Lemieux-Dudon, B., Loulergue, L., Masson-Delmotte, V., Narcisi, B., Petit, J.-R., Raisbeck, G., Raynaud, D., Ruth, U., Schwander, J., Severi, M., Spahni, R., Steffensen, J. P., Svensson, A., Udisti, R., Waelbroeck, C., and Wolff, E.: The EDC3 chronology for the EPICA Dome C ice core, Clim. Past, 3, 485–497, doi:10.5194/cp-3-485-2007, 2007b.

Petit, J. R., Jouzel, J., Raynaud, D., Barkov, N. I., Barnola, J.-M., Basile, I., Bender, M., Chappellaz, J., Davis, M., Delaygue, G., Delmotte, M., Kotlyakov, V. M., Legrand, M., Lipenkov, V. Y., Lorius, C., Pépin, L., Ritz, C., Saltzman, E., and Stievenard, M.: Climate and atmospheric history of the past 420,000 years from the Vostok ice core, Antarctica, Nature, 399, 429–436, doi:10.1038/20859, 1999.

Raisbeck, G. M., Yiou, F., Fruneau, M., and Loiseaux, J. M.: Beryllium-10 mass spectrometry with a cyclotron, Science, 202, 215–217, doi:10.1126/science.202.4364.215, 1978.

Raisbeck, G. M., Yiou, F., Fruneau, M., Loiseaux, J. M., Lieuvin, M., and Ravel, J. C.: Cosmogenic $^{10}Be/^{7}Be$ as a probe of atmospheric transport processes, Geophys. Res. Lett., 8, 1015–1018, doi:10.1029/GL008i009p01015, 1981a.

Raisbeck, G. M., Yiou, F., Fruneau, M., Loiseaux, J. M., Lieuvin, M., Ravel, J. C., and Lorius, C.: Cosmogenic ^{10}Be concentrations in Antarctic ice during the past 30,000 years, Nature, 292, 825, doi:10.1038/292825a0, 1981b.

Raisbeck, G. M., Yiou, F., Bourlès, D., Lorius, C., and Jouzel, J.: Evidence for two intervals of enhanced ^{10}Be deposition in Antarctic ice during the last glacial period, Nature, 326, 273–277, doi:10.1038/326273a0, 1987.

Raisbeck, G. M., Yiou, F., Jouzel, J., and Stocker, T. F.: Direct north-south synchronization of abrupt climate change record in ice cores using Beryllium 10, Clim. Past, 3, 541–547, doi:10.5194/cp-3-541-2007, 2007.

Raynaud, D., Lipenkov, V., Lemieux-Dudon, B., Duval, P., Loutre, M.-F., and Lhomme, N.: The local insolation signature of air content in Antarctic ice. A new step toward an absolute dating of ice records, Earth Planet. Sc. Lett., 261, 337–349, doi:10.1016/j.epsl.2007.06.025, 2007.

Risi, C., Bony, S., Vimeux, F., and Jouzel, J.: Water-stable isotopes in the LMDZ4 general circulation model: model evaluation for present-day and past climates and applications to climatic interpretations of tropical isotopic records, J. Geophys. Res., 115, D12118, doi:10.1029/2009JD013255, 2010.

Ritz, C.: Un modèle thermo-mécanique d'évolution pour le bassin glaciaire Antarctique Vostok-Glacier Byrd: Sensibilité aux valeurs des paramètres mal connus, Ph.D. thesis, Université Joseph Fourier – Grenoble I, 1992.

Roeckner, E., Brokopf, R., Esch, M., Giorgetta, M., Hagemann, S., Kornblueh, L., Manzini, E., Schlese, U., and Schulzweida, U.: Sensitivity of simulated climate to horizontal and vertical resolution in the ECHAM5 atmosphere model, J. Climate, 19, 3771, doi:10.1175/JCLI3824.1, 2006.

Salamatin, A. N., Lipenkov, V. Y., Barkov, N. I., Jouzel, J., Petit, J. R., and Raynaud, D.: Ice core age dating and paleothermometer calibration based on isotope and temperature profiles from deep boreholes at Vostok Station (East Antarctica), J. Geophys. Res., 103, 8963–8977, doi:10.1029/97JD02253, 1998.

Schäfer-Neth, C. and Paul, A.: Gridded Global LGM SST and Salinity Reconstruction, IGBP PAGES/World Data Center for Paleoclimatology, Boulder. Data Contribution Series #2003-046.,

NOAA/NGDC Paleoclimatology Program, Boulder CO, USA, available at: ftp://ftp.ncdc.noaa.gov/pub/data/paleo/contributions_by_author/paul2003, 2003.

Schmidt, G. A., Legrande, A. N., and Hoffmann, G.: Water isotope expressions of intrinsic and forced variability in a coupled ocean-atmosphere model, J. Geophys. Res., 112, D10103, doi:10.1029/2006JD007781, 2007.

Sime, L. C., Tindall, J. C., Wolff, E. W., Connolley, W. M., and Valdes, P. J.: Antarctic isotopic thermometer during a CO_2 forced warming event, J. Geophys. Res., 113, D24119, doi:10.1029/2008JD010395, 2008.

Sime, L. C., Wolff, E. W., Oliver, K. I. C., and Tindall, J. C.: Evidence for warmer interglacials in East Antarctic ice cores, Nature, 462, 342–345, doi:10.1038/nature08564, 2009.

Singer, B. S., Guillou, H., Jicha, B. R., Laj, C., Kissel, C., Beard, B. L., and Johnson, C. M.: $^{40}\mathrm{Ar}/^{39}\mathrm{Ar}$, K-Ar and $^{230}\mathrm{Th} - ^{238}\mathrm{U}$ dating of the Laschamp excursion: a radioisotopic tie-point for ice core and climate chronology, Earth Planet. Sc. Lett., 286, 80–88, doi:10.1016/j.epsl.2009.06.030, 2009.

Suwa, M. and Bender, M. L.: Chronology of the Vostok ice core constrained by $\mathrm{O}_2/\mathrm{N}_2$ ratios of occluded air, and its implication for the Vostok climate records, Quaternary Sci. Rev., 27, 1093–1106, doi:10.1016/j.quascirev.2008.02.017, 2008.

Taylor, K. E., Balaji, V., Hankin, S., Juckes, M., Lawrence, B., and Pascoe, S.: CMIP5 Data Reference Syntax (DRS) and Controlled Vocabularies, version 1.3.1, available at: http://cmip-pcmdi.llnl.gov/cmip5/docs/cmip5_data_reference_syntax.pdf, 2012.

Thouveny, N., Bourlès, D. L., Saracco, G., Carcaillet, J. T., and Bassinot, F.: Paleoclimatic context of geomagnetic dipole lows and excursions in the Brunhes, clue for an orbital influence on the geodynamo?, Earth Planet. Sc. Lett., 275, 269–284, doi:10.1016/j.epsl.2008.08.020, 2008.

van Ommen, T. D. and Morgan, V.: Calibrating the ice core paleothermometer using seasonality, J. Geophys. Res., 102, 9351–9358, doi:10.1029/96JD04014, 1997.

Veres, D., Bazin, L., Landais, A., Toyé Mahamadou Kele, H., Lemieux-Dudon, B., Parrenin, F., Martinerie, P., Blayo, E., Blunier, T., Capron, E., Chappellaz, J., Rasmussen, S. O., Severi, M., Svensson, A., Vinther, B., and Wolff, E. W.: The Antarctic ice core chronology (AICC2012): an optimized multi-parameter and multi-site dating approach for the last 120 thousand years, Clim. Past, 9, 1733–1748, doi:10.5194/cp-9-1733-2013, 2013.

Vimeux, F., Cuffey, K. M., and Jouzel, J.: New insights into Southern Hemisphere temperature changes from Vostok ice cores using deuterium excess correction, Earth Planet. Sc. Lett., 203, 829–843, doi:10.1016/S0012-821X(02)00950-0, 2002.

Wagner, W. and Pruß, A.: The IAPWS formulation 1995 for the thermodynamic properties of ordinary water substance for general and scientific use, J. Phys. Chem. Ref. Data, 31, 387, doi:10.1063/1.1461829, 2002.

Watanabe, O., Jouzel, J., Johnsen, S., Parrenin, F., Shoji, H., and Yoshida, N.: Homogeneous climate variability across East Antarctica over the past three glacial cycles, Nature, 422, 509–512, doi:10.1038/nature01525, 2003.

Werner, M., Langebroek, P. M., Carlsen, T., Herold, M., and Lohmann, G.: Stable water isotopes in the ECHAM5 general circulation model: Toward high-resolution isotope modeling on a global scale, J. Geophys. Res., 116, D15109, doi:10.1029/2011JD015681, 2011.

Yiou, F., Raisbeck, G. M., Bourles, D., Lorius, C., and Barkov, N. I.: ^{10}Be in ice at Vostok Antarctica during the last climatic cycle, Nature, 316, 616–617, doi:10.1038/316616a0, 1985.

Yiou, F., Raisbeck, G. M., Baumgartner, S., Beer, J., Hammer, C., Johnsen, S., Jouzel, J., Kubik, P. W., Lestringuez, J., Stiévenard, M., Suter, M., and Yiou, P.: Beryllium 10 in the Greenland Ice Core Project ice core at Summit, Greenland, J. Geophys. Res., 102, 26783–26794, doi:10.1029/97JC01265, 1997.

Table 1. List of all simulations used in this study (see Fig. 3). The ensemble member (r$\langle N \rangle$i$\langle M \rangle$p$\langle L \rangle$) formatted as shown below (e.g. "r3i1p21" with r for "realization", i for "initialization method indicator" and p for "perturbed physics") distinguishes among closely related simulations by a single model (Taylor et al., 2012). The reference given in brackets next to the ensemble number in columns 4 and 5 is the name of the simulation used on Fig. 3.

			CMIP5 experiment Model *ensemble member* used (r$\langle N \rangle$i$\langle M \rangle$p$\langle L \rangle$)	
Institute	Model	Model institution	0k piControl	21k lgm
CNRM-CERFACS	CNRM-CM5	Centre National de Recherches Météorologiques/Centre Européen de Recherche et Formation Avancée en Calcul Scientifique, France	r1i1p1 (CNRM-CM5)	r1i1p1 (CNRM-CM5)
NASA-GISS	GISS-E2-R	NASA Goddard Institute for Space Studies, US	r1i1p142 (GISS-E2-R_p150) r1i1p142 (GISS-E2-R_p151)	r1i1p150 (GISS-E2-R_p150) r1i1p151 (GISS-E2-R_p151)
IPSL	IPSL-CM5A-LR	Institut Pierre-Simon Laplace, France	r1i1p1 (IPSL-CM5A-LR)	r1i1p1 (IPSL-CM5A-LR)
LASC-CESS	FGOALS-g2	LASG, Institute of Atmospheric Physics, Chinese Academy of Sciences and CESS, Tsinghua University, China	r1i1p1 (FGOALS-g2)	r1i1p1 (FGOALS-g2)
MIROC	MIROC-ESM	Japan Agency for Marine-Earth Science and Technology, Atmosphere and Ocean Research Institute (The University of Tokyo), and National Institute for Environmental Studies, Japan	r1i1p1 (MIROC-ESM)	r1i1p1 (MIROC-ESM)
MPI-M	MPI-ESM-P	Max Planck Institute for Meteorology, Hamburg, Germany	r1i1p1 (MPI-ESM-P_p1) r1i1p1 (MPI-ESM-P_p2)	r1i1p1 (MPI-ESM-P_p1) r1i1p2 (MPI-ESM-P_p1)
MRI	MRI-CGCM3	Meteorological Research Institute, Tsukuba, Japan	r1i1p1 (MRI-CGCM3)	r1i1p1 (MRI-CGCM3)
NCAR	CCSM4	National Center for Atmospheric Research, US/Dept. of Energy/NSF	r1i1p1 (CCSM4_r1) r2i1p1 (CCSM4_r2)	r1i1p1 (CCSM4_r1) r2i1p1 (CCSM4_2)

Table 2. List of markers used to constrain EDC and Vostok ice cores between 269 and 355 ka for the AICC2012 chronology. References ("Ref."): (1) Suwa and Bender (2008) (2) Lipenkov et al. (2011) (3) Raynaud et al. (2007) (4) Bazin et al. (2013).

Vostok age markers	Depth	Age	Uncertainty	Type of markers	Ref.
Ice age markers	2882.1	275 200	4000	$\delta O_2/N_2$	1
	2883.02	275 950	6343	air content	2
	2912.1	286 300	4000	$\delta O_2/N_2$	1
	2962.7	296 800	4000	$\delta O_2/N_2$	1
	3005.6	307 700	4000	$\delta O_2/N_2$	1
	3011	307 950	6424	air content	2
	3040.7	319 200	4000	$\delta O_2/N_2$	1
	3043.04	318 950	6308	air content	2
	3080.5	330 000	4000	$\delta O_2/N_2$	1
	3130.6	339 700	4000	$\delta O_2/N_2$	1
	3145.95	346 950	6527	air content	2
	3157.1	349 200	4000	$\delta O_2/N_2$	1
Gas age markers	2887	272 900	6000	$\delta^{18}O_{atm}$	1
	2947.6	285 900	6000	$\delta^{18}O_{atm}$	1
	2990.3	297 500	6000	$\delta^{18}O_{atm}$	1
	3026.9	308 300	6000	$\delta^{18}O_{atm}$	1
	3062.5	318 300	6000	$\delta^{18}O_{atm}$	1
	3101.4	329 000	6000	$\delta^{18}O_{atm}$	1
	3146.2	340 300	6000	$\delta^{18}O_{atm}$	1
	3173.8	351 000	6000	$\delta^{18}O_{atm}$	1
EDC age markers					
Ice age markers	2500.25	306 950	6652	air content	3
	2510.75	318 950	6242	air content	3
	2610.8	346 950	7120	air content	3
Stratigraphic links between EDC and Vostok					
	Depth EDC	Depth Vostok	Uncertainty	Type of markers	Ref.
	2419.34	2911.06	1500	CH_4	4
	2451.33	2954.61	1500	CH_4	4
	2501.4	3018.01	1500	CH_4	4
	2521.2	3051.5	1500	CH_4	4
	2544.83	3079.41	1500	CH_4	4
	2583.9	3123.5	1500	CH_4	4
	2613	3162.8	1500	CH_4	4

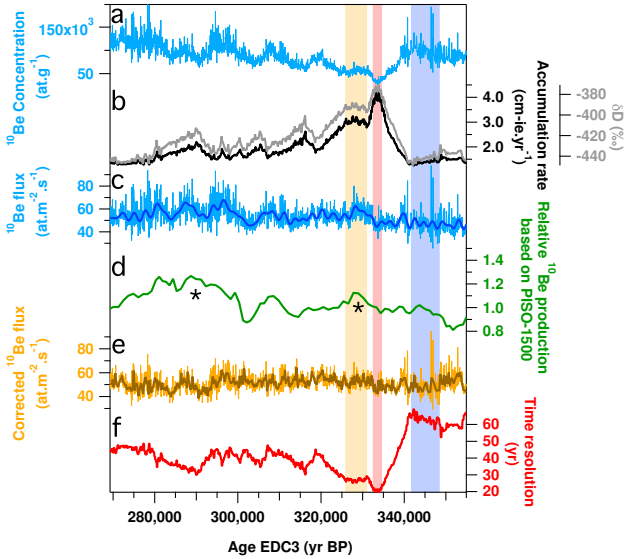

Figure 1. High resolution $^{10}\mathrm{Be}$ data between 2384 and 2627 m deep (269–355 ka on EDC3 age scale). **(a)** Raw $^{10}\mathrm{Be}$ concentrations ($\mathrm{at\,g^{-1}}$). **(b)** In grey, δD profile at EDC including the interglacial period MIS 9.3 (Jouzel et al., 2007). In black, the accumulation rate of the site ($\mathrm{cm\,ie\,yr^{-1}}$) (Parrenin et al., 2007b). The light yellow and light red areas show the plateau during MIS 9.3 at the same isotopic level than PI and the MIS 9.3 optimum warmer than PI. The light blue area corresponds to the MIS 10 glacial maximum just before the Termination IV. **(c)** Calculated $^{10}\mathrm{Be}$ flux using EDC3 accumulation rate. The light-blue curve corresponds to raw data, the bold-blue curve is the low-pass filtered $^{10}\mathrm{Be}$ flux ($1/2000\,\mathrm{yr^{-1}}$). **(d)** $^{10}\mathrm{Be}$ production based on paleointensity record PISO-1500 (Channell et al., 2009) on EDC3 age scale and calculated using calculations of Masarik and Beer (2009). The asterisks show the possible correlation with proposed geomagnetic events, Portuguese Margin (~ 290 ka) and Calabrian Ridge 1 (~ 320 ka). **(e)** Raw and 100 yr resampled $^{10}\mathrm{Be}$ flux corrected by PISO-1500. **(f)** Time resolution of the $^{10}\mathrm{Be}$ profile (difference between the n and $n+1$ sample ages).

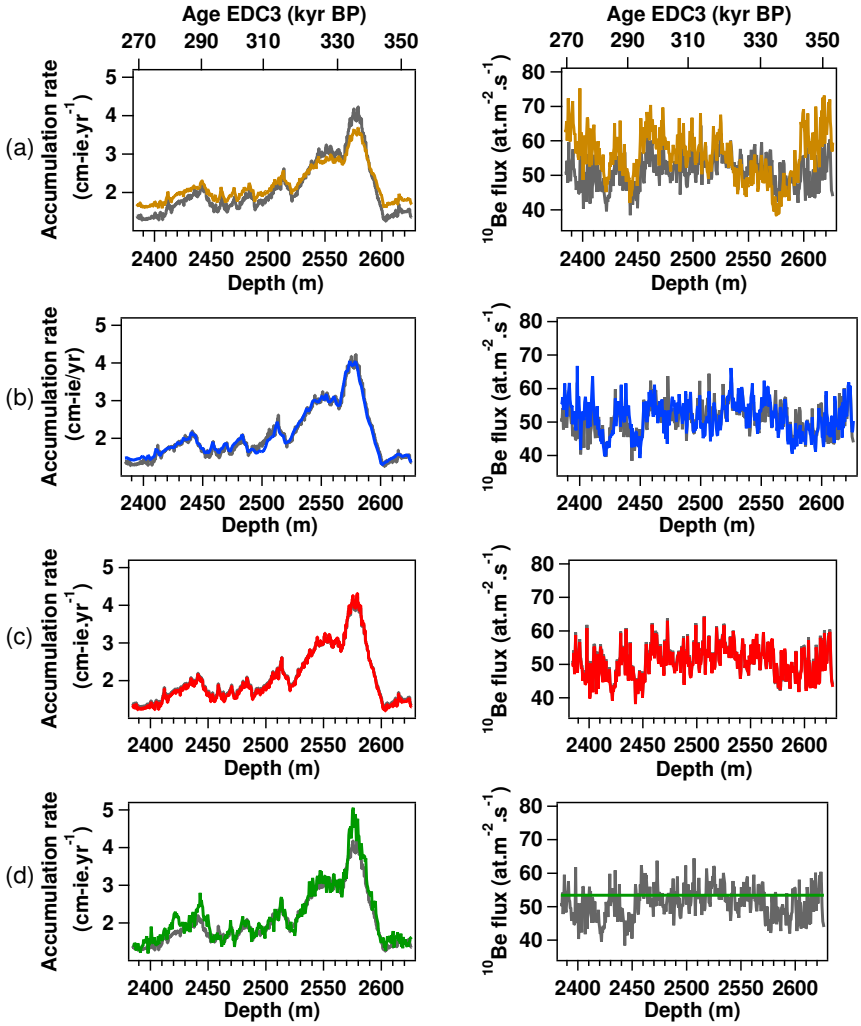
Age EDC3 (kyr BP)
270 290 310 330 350
(a)
(b)
(c)
(d)
Accumulation rate (cm-ie.yr-1)
Accumulation rate (cm-ie/yr)
10Be flux (at.m-2.s-1)
2400 2450 2500 2550 2600
Depth (m)

Figure 2. Several accumulation rate reconstructions (left column) and the corresponding $^{10}\mathrm{Be}$ flux corrected by PISO-1500 (right column) discussed in Sect. 3 (colored curves). The EDC3 reconstruction from Parrenin et al. (2007a, b) is shown in grey for comparison. **(a)** Saturation vapour pressure formulation **(b)** Application of the AICC2012 chronology on the $^{10}\mathrm{Be}$ record **(c)** Optimization of the interglacial–glacial amplitude coefficient (β) by minimization of the variance of the $^{10}\mathrm{Be}$ flux corrected for past variations of geomagnetic field intensity (red curves) **(d)** Accumulation rate assuming a constant $^{10}\mathrm{Be}$ flux (fixed at 53.44 $\mathrm{at\,m^{-2}\,s^{-1}}$ over the whole period).

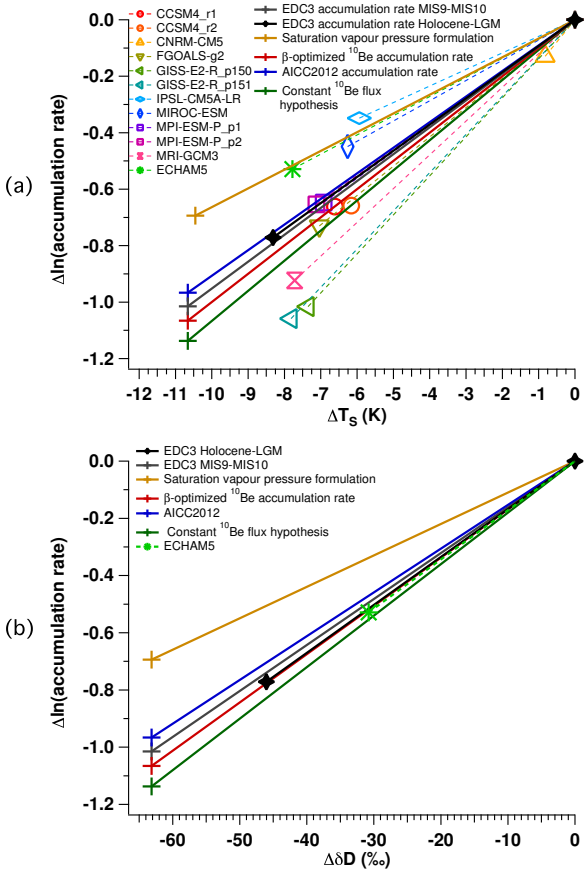

Figure 3. (a) Accumulation rate vs. temperature change between the LGM and PI for 12 different simulations and comparison with the relationships from EDC3 (last deglaciation and MIS 9.3) and our reconstructions (average during the glacial and the interglacial period). **(b)** Accumulation rate vs. δD change for both ice core data and ECHAM5 simulation results.